

Molecular imaging correlates of tryptophan metabolism via the kynurenine pathway in human meningiomas

Edit Bosnyák, David O. Kamson, Anthony R. Guastella, Kaushik Varadarajan, Natasha L. Robinette, William J. Kupsky, Otto Muzik, Sharon K. Michelhaugh, Sandeep Mittal[†], and Csaba Juhász[†]

Department of Pediatrics, Wayne State University, Detroit, Michigan (E.B., D.O.K., O.M., C.J.); Department of Neurology, Wayne State University, Detroit, Michigan (C.J.); Department of Neurosurgery, Wayne State University, Detroit, Michigan (A.R.G., K.V., S.K.M., S.M.); Department of Oncology, Wayne State University, Detroit, Michigan (A.R.G., S.M.); Department of Radiology, Wayne State University, Detroit, Michigan (N.L.R., O.M.); Department of Pathology, Wayne State University, Detroit, Michigan (W.J.K.); PET Center, Children's Hospital of Michigan, Detroit, Michigan (E.B., D.O.K., O.M., C.J.); Karmanos Cancer Institute, Detroit, Michigan (N.L.R., W.J.K., S.M., C.J.)

Corresponding Author: Csaba Juhász, MD, PhD, PET Center and Translational Imaging Laboratory, Children's Hospital of Michigan, Departments of Neurology and Pediatrics, Wayne State University School of Medicine, 3901 Beaubien Street, Detroit, MI 48201 (juhasz@pet.wayne.edu).

[†]These authors contributed equally to this manuscript.

Background. Increased tryptophan metabolism via the kynurenine pathway (KP) is a key mechanism of tumoral immune suppression in gliomas. However, details of tryptophan metabolism in meningiomas have not been elucidated. In this study, we evaluated in vivo tryptophan metabolism in meningiomas and compared it with gliomas using α -[¹¹C]-methyl-L-tryptophan (AMT)-PET. We also explored expression patterns of KP enzymes in resected meningiomas.

Methods. Forty-seven patients with MRI-detected meningioma ($n = 16$) and glioma ($n = 31$) underwent presurgical AMT-PET scanning. Tumoral AMT uptake and tracer kinetic parameters (including K and k_3' evaluating unidirectional uptake and trapping, respectively) were measured, correlated with meningioma grade, and compared between meningiomas and gliomas. Patterns of KP enzyme expression were assessed by immunohistochemistry in all meningiomas.

Results. Meningioma grade showed a positive correlation with AMT k_3' tumor/cortex ratio ($r = 0.75$, $P = .003$), and this PET parameter distinguished grade I from grade II/III meningiomas with 92% accuracy. Kinetic AMT parameters could differentiate meningiomas from both low-grade gliomas (97% accuracy by k_3' ratios) and high-grade gliomas (83% accuracy by K ratios). Among 3 initial KP enzymes (indoleamine 2,3-dioxygenase 1/2, and tryptophan 2,3-dioxygenase 2 [TDO2]), TDO2 showed the strongest immunostaining, particularly in grade I meningiomas. TDO2 also showed a strong negative correlation with AMT k_3' ratios ($P = .001$).

Conclusions. PET imaging of tryptophan metabolism can provide quantitative imaging markers for differentiating grade I from grade II/III meningiomas. TDO2 may be an important driver of in vivo tryptophan metabolism in these tumors. These results can have implications for pharmacological targeting of the KP in meningiomas.

Keywords: glioma, indoleamine 2,3-dioxygenase (IDO), meningioma, positron emission tomography (PET), tryptophan 2,3-dioxygenase (TDO).

Meningiomas are the most frequently diagnosed primary brain tumors in adults, accounting for approximately one-third of all primary brain tumors.¹ They occur about twice as often in women as in men. The WHO classifies 3 grades of meningiomas based on histological criteria (grade I [benign], grade II [atypical], and grade III [anaplastic]) that occur in decreasing order of frequency. Initial treatment often includes surgery, although watchful waiting is also an option in small, asymptomatic meningiomas. Surgical morbidity is considerably higher in older

patients with asymptomatic tumors; as such, close follow-up of small low-grade meningiomas may be the best strategy.² Radiation therapy is frequently recommended after surgery for high-grade meningiomas, although it may not be completely efficacious. Chemotherapeutic options still remain very limited. The 5-year recurrence rate after surgery is 12% for grade I, 41% for grade II, and 56% for grade III meningiomas.

Meningiomas are usually readily identified by clinical MRI, where these tumors typically appear as a solid, extra-axial,

Received 11 February 2015; accepted 6 May 2015

© The Author(s) 2015. Published by Oxford University Press on behalf of the Society for Neuro-Oncology. All rights reserved. For permissions, please e-mail: journals.permissions@oup.com.

contrast-enhancing mass. However, conventional MRI has limited ability to differentiate tumor tissue from nonspecific tissue changes, and it is not able to accurately differentiate low-grade from high-grade meningiomas.³ Advanced MR imaging techniques as well as PET have been evaluated for characterization of newly diagnosed meningiomas.^{4,5} On magnetic resonance spectroscopy (¹H-MRS), meningiomas show a high level of choline and reduction of N-acetyl-aspartate and creatine, while lipid and alanine peaks may be seen occasionally. Extensive necrosis or fatty degeneration may result in increased lipid content.^{6–8} However, ¹H-MRS is not useful for detecting small tumors and evaluating lesions near the ventricles or scalp, calcified structures, and hemorrhagic tumors.⁹ Perfusion-weighted imaging can provide additional information regarding the vascularity of meningiomas and may help differentiate low-grade from high-grade tumors.¹⁰ In contrast, diffusion-weighted imaging was found to have a limited value for meningioma grading in a large study.¹¹

Clinical PET using 2-deoxy-2-[¹⁸F]fluoro-D-glucose (FDG) can distinguish low-grade from high-grade gliomas with moderate accuracy¹²; however, it has a limited role in differentiating meningiomas of various histological grades. A limited number of studies have assessed the use of various amino acid PET tracers as a clinically useful alternative for evaluation of meningiomas.^{5,13,14}

Tumoral metabolism of the essential amino acid tryptophan can be studied by α-[¹⁴C]-methyl-L-tryptophan (AMT)-PET. Tryptophan (and also AMT) is transported in brain tumor tissue via the large neutral amino acid transporter (LAT1).^{15–17} AMT, unlike tryptophan, is not incorporated into proteins,¹⁸ but both can be metabolized via the immunomodulatory kynurenine pathway (KP), which plays a key role in tumoral immune tolerance.^{19–23} In our recent PET studies, we demonstrated increased transport and metabolic rates of tryptophan in a variety of gliomas and glioneuronal tumors regardless of MRI contrast enhancement.^{24–26} The same tumors also showed variable expression of LAT1 as well as indoleamine 2,3-dioxygenase (IDO; a key enzyme of the KP) on immunohistochemistry (IHC).^{15,21} We also found a positive correlation between glioma proliferative activity and tryptophan net transport rates assessed by AMT-PET kinetic analysis.²⁷ High AMT uptake in patients with suspected recurrent glioma has a strong, independent prognostic value for poor survival.²⁸ In a recent study of freshly resected meningiomas, we reported expression of both LAT1 and IDO, suggesting an active KP.²⁹ However, conversion of tryptophan to kynurenine can be mediated by at least 3 distinct enzymes: IDO1, IDO2, and tryptophan 2,3-dioxygenase 2 (TDO2), all of which could be targeted by inhibitors to alleviate tumoral immune resistance to enhance the effects of chemo- or immunotherapy.^{30,31}

In the present study, we used AMT-PET with detailed tracer kinetic analysis to evaluate mechanisms and potential clinical significance of abnormal tryptophan uptake and metabolism in WHO grade I–III meningiomas. We assessed if AMT-PET could differentiate between low-grade versus high-grade meningiomas and/or predict meningioma proliferative activity. We also determined whether AMT static uptake and/or kinetic variables are able to accurately differentiate meningiomas from low-grade and high-grade gliomas. Finally, we studied tumoral expression of enzymes of the KP (including IDO1, IDO2, and TDO2

as well as 2 downstream enzymes; see Fig. 1) in all resected meningiomas and correlated enzyme expression data with in vivo kinetic parameters measured by PET. The goal of these latter studies was to better understand the mechanisms of abnormal tryptophan metabolism in meningiomas and explore the feasibility of targeting KP enzymes by inhibitors in these tumors.

Materials and Methods

Patient Population

The study population comprised 47 patients (26 males; age range: 10–91 y) who underwent presurgical neuroimaging with high-resolution MRI and AMT-PET scan for evaluation of suspected (intra- or extra-axial) brain tumor followed by microsurgical tumor resection. Meningioma was confirmed in 16 patients (mean age: 56.9 y), and WHO grade II or III glioma was verified in 31 patients (mean age: 42.9 y) by histopathology. In the meningioma subgroup, 10 patients had a grade I tumor, while 6 harbored a high-grade meningioma (grade II: *n* = 5; grade III: *n* = 1). In the glioma subgroup, 12 patients had grade II oligodendroglioma, 4 patients had grade II mixed oligoastrocytoma, and 5 patients had grade II astrocytoma. Ten additional patients had a grade III glioma (5 astrocytoma, 3 mixed oligoastrocytoma, 2 oligodendroglioma). All tumors had a maximum diameter of at least 15 mm (range 15–90 mm, mean: 45 mm). The study was approved by the

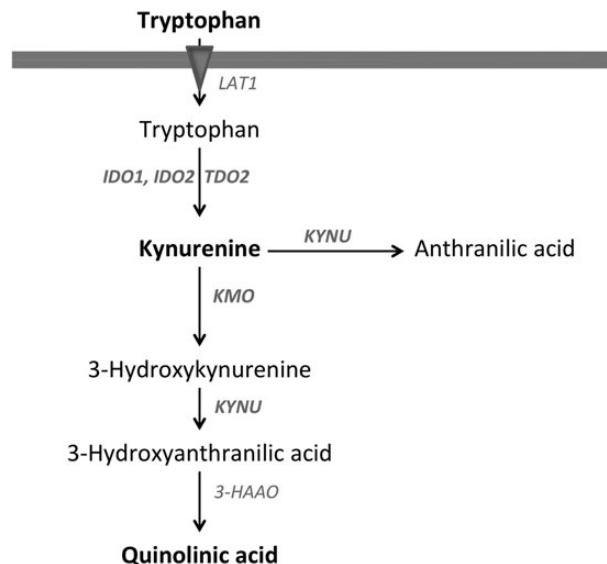


Fig. 1. The key steps and enzymes of tryptophan transport and metabolism by the kynurenine pathway (KP). Large neutral amino acid transporter 1 (LAT1) is the main transporter carrying tryptophan from blood into the tissue. Key enzymes of the KP: IDO (indoleamine 2,3-dioxygenase), TDO (tryptophan 2,3-dioxygenase), KMO (kynurenine 3-monooxygenase), KYNU (kynureninase), and 3-HAAO (3-hydroxyanthranilic acid oxygenase). Tumoral conversion of tryptophan to kynurenine can be mediated by at least 3 distinct enzymes: IDO1, IDO2 and TDO2. Kynurenine can be further metabolized by 2 main enzymes (KMO, KYNU) to downstream metabolites including quinolinic acid. The 5 enzymes whose abundance was evaluated in this study are bolded on the figure.

Institutional Review Board of Wayne State University, and written informed consent was obtained from all participants.

AMT-Positron Emission Tomography Scanning Protocol

The AMT-PET studies were performed using a Siemens EXACT/HR whole-body positron emission tomograph located at the PET Center of the Children's Hospital of Michigan in Detroit. The PET image in-plane resolution was 7.5 ± 0.4 mm at full-width half-maximum and 7.0 ± 0.5 mm at full-width half-maximum in the axial direction. The AMT tracer was synthesized using a high-yield procedure as previously outlined.³² The procedure for AMT-PET scanning has been described in detail elsewhere.²⁴ In short, following a 6 hour fast, a slow bolus of AMT (3.7 MBq/kg) was injected intravenously over 2 minutes. For collection of timed blood samples, a second venous line was established. In the initial 20 minutes of the scan following tracer injection, a dynamic PET scan of the heart was performed to obtain the blood input function from the left cardiac ventricle noninvasively. The blood input function was continued beyond these initial 20 minutes by using venous blood samples (0.5 mL/sample, collected at 20, 30, 40, 50, and 60 min after AMT injection). At 25 minutes after tracer injection, a dynamic emission scan of the brain (7×5 min) was obtained. Measured attenuation correction, scatter, and decay correction were applied to all PET images.

Magnetic Resonance Imaging Protocol

Diagnostic MRI scans with routine post-gadolinium T1 (T1-Gad), T2-weighted, and fluid-attenuated inversion recovery

(FLAIR) axial images acquired closest in time (typically within 2 wk) to the AMT-PET were used in the study. MRI was performed on one of 3 3T scanners using similar parameters: (i) Siemens MAGNETOM Trio TIM; (ii) GE Signa HDxt; or (iii) Philips Achieva TX.

AMT-Positron Emission Tomography Image Processing and Analysis

For visualization of AMT uptake in the brain, averaged activity images 30–55 minutes post injection were created and converted to an AMT standardized uptake value (SUV) image. For quantification of AMT accumulation, a Patlak graphical analysis was performed using the dynamic brain PET images and blood input function.^{24,33} This approach provides 2 kinetic parameters. The y intercept of the Patlak plot (Fig. 2) yields the tracer's apparent volume of distribution (VD'), which is tightly correlated with VD values derived from compartmental analysis [$VD = K_1/(k_2+k_3)$], where K_1 (mL/g/min) represents the forward, k_2 (min^{-1}) represents the reverse combined transport of AMT across the blood vessel, interstitial space, and cell membrane into the cytoplasm, and k_3 (min^{-1}) represents the metabolic rate constant that reflects tracer accumulation in the metabolic (irreversible) compartment (in case of tumoral tryptophan metabolism via the KP).³⁴ Therefore, AMT VD' values are indicative of the net transport of tryptophan into the tissue of interest (tumor or cortex). The slope of the Patlak plot reflects the unidirectional uptake of tracer into the tissue (K-complex) and correlates with tryptophan metabolism via the serotonin synthesis pathway in cortex.^{19,35} In brain tumors with no evidence of serotonin synthesis, the most likely mechanism of

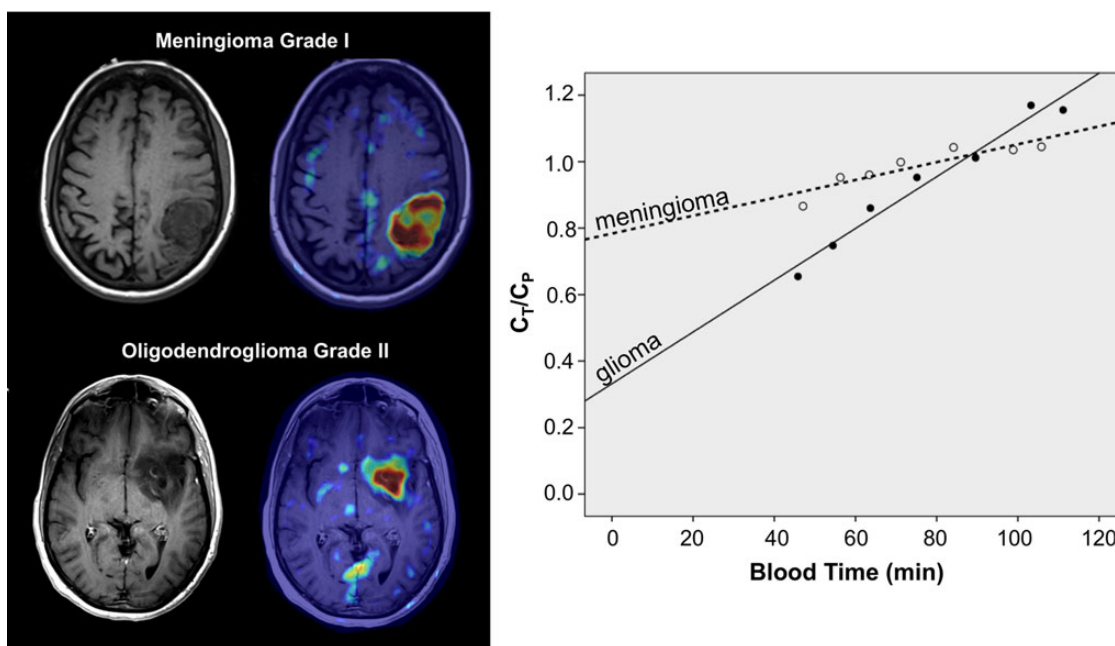


Fig. 2. AMT-PET summed images and corresponding Patlak curves of a meningioma and a low-grade glioma. Both tumors showed high AMT standardized uptake values but very different AMT kinetics. The slope of the glioma curve was much steeper than the meningioma curve, indicating higher K value. In contrast, the y intercept was much lower in the glioma, indicating lower volume of distribution (VD'). The x axis represents transformed time ("blood time") in minutes. C_t = tracer concentration in tumor tissue; C_p = tracer concentration in plasma.

an increase in AMT K-complex is tumoral accumulation in the form of either unmetabolized AMT or kynurenine metabolites.¹⁹ In addition, the ratio between K and VD' yields parameter k_3' , an estimate of the k_3 parameter that characterizes the irreversible trapping of AMT, presumably due to enzymatic conversion to α -methyl-L-kynurenine. The advantages and limitations of using these kinetic AMT-PET parameters have been discussed previously.^{24,35,36,38}

For image analysis, the 3D Slicer 3.6.3 software suite was used (<http://www.slicer.org>)³⁷ as described previously.²⁸ First, a transformation matrix was created by co-registration of the summed AMT-PET images to the T1-Gad volumetric image volumes (magnetization-prepared rapid gradient-echo [MPRAGE] protocol on Siemens or MPRAGE-equivalent sequence on GE and Philips scanners) as well as FLAIR images using the Fast Rigid Registration module.³⁸ This transformation matrix was then applied to the summed AMT-PET image and to the dynamic AMT-PET images loaded via the 4D image module of 3D Slicer. Following fusion of the summed AMT-PET with MR images, the largest orthogonal diameters and maximum tumor area on T1-Gad (or T2/FLAIR images, if no enhancement was seen) were measured. Regions of interest (ROIs) were drawn on the tumor mass in tumor regions with MPRAGE contrast enhancement and/or T2/FLAIR signal changes on MRI, and the ROIs were then applied on the co-registered AMT SUV as well dynamic PET images. As a reference (background) region, at least 3 ROIs were drawn on the homotopic cortex contralateral to the tumor, and the values from these ROIs were averaged. The following AMT-PET parameters were assessed in the ROI showing the highest AMT uptake: tumor SUV, K, VD', and k_3' , as well as the tumor/cortex ratios for all 4 parameters.

Immunohistochemistry Studies of Resected Tumors

Five key enzymes of the KP (Fig. 1) were assessed by IHC in all meningioma samples ($n = 16$). Tissue sections (5 μm) were cut from the selected formalin-fixed paraffin-embedded tumor blocks and mounted on charged slides for IHC analysis using specific antibodies for IDO1 (cat# NBP1-87702, Novus Biologicals), IDO2 (cat# OAAB08672, Aviva Systems Biology), TDO2 (cat# NBP2-13424, Novus Biologicals), kynurenine 3-monooxygenase (KMO; cat# 60029-1-Ig, Proteintech Group), and kynureninase (KYNU; cat# NBP1-56545, Novus Biologicals). Standard IHC protocols using avidin-biotin complex were completed using Vectastain Elite ABC kits (Vector Labs). Briefly, after deparaffinizing and hydrating with phosphate-buffered saline (pH 7.4), the sections were pretreated with hydrogen peroxide (3%) for 10 minutes to remove endogenous peroxidase activity, followed by antigen retrieval via steam bath for 20 minutes in citrate buffer (pH 6.0). Primary antibody was applied (1:100), followed by washing and incubation with the biotinylated secondary antibody for 30 minutes at room temperature. After another set of washes, avidin-peroxidase was added, allowing for detection of antibody binding using the substrate diaminobenzidine. Sections were counterstained with Mayer hematoxylin, dehydrated, and mounted for microscopic examination. The immunostaining results for each studied enzyme were assessed by scoring staining intensity as follows: 0 = no staining; 1 = mild staining; 2 = moderate staining; 3 = strong staining in at least 3 representative 20 \times magnification fields of view of all

selected tumor samples by 2 of the investigators. The proliferation index was assessed by Ki-67 nuclear immunostaining.

Statistical Analysis

AMT-PET parameters and tumor size (maximum area) were compared between the meningioma and glioma subgroups using unpaired *t* tests. The optimal cutoff threshold of the best AMT-PET parameter to differentiate meningiomas from gliomas (both low-grade and high-grade, separately) was established by a receiver operating characteristics (ROC) analysis, and the differentiating accuracy of the parameter was calculated. Further, AMT-PET variables in the meningioma group were correlated with patient age, tumor size, and histological grade as well as the tumor proliferative index expressed as the Ki-67 labeling index (%), using Pearson's correlations. To test the accuracy of the best PET parameter (k_3') to differentiate low-grade and high-grade meningiomas, a ROC analysis was performed again. Confidence intervals for the area under the curve (AUC) and accuracy using the optimum threshold from the ROC were calculated using bootstrapping with 10 000 bootstrap replicates.

To determine the accuracy of the best AMT-PET parameter for differentiating grade I versus grade II-III meningiomas, an optimal cutoff threshold was again established using ROC analysis, and the sensitivity and specificity of the parameter for differentiating these 2 meningioma grade groups were calculated. Immunostaining scores of the different KP enzymes were compared using a Wilcoxon signed-rank test; specifically, the 3 initial enzymes (IDO1, IDO2, and TDO2) were compared with each other, and the 2 downstream enzymes (KMO, KYNU) were also compared with each other. Enzyme expression scores between low-grade and high-grade meningiomas were compared using the Mann-Whitney *U* test. Finally, we correlated KP enzyme immunostaining scores with AMT-PET kinetic parameters using the Spearman rank test. Statistical analysis was performed using IBM SPSS Statistics, version 19.0 (except for bootstrapping, for which the pROC package in R was used³⁹). A *P* value <.05 was considered to be significant.

Results

All 16 meningiomas showed increased AMT uptake (high SUV value) as compared with contralateral homotopic cortex; the mean tumor/cortex SUV ratio was 1.61 (range: 1.14–2.12) (see Table 1). Also, all meningiomas showed high VD' values, and the mean tumor/cortex VD'-ratio was 2.60 (range: 1.6–4.4), indicating high net tryptophan transport from blood to tumor. Tumor/cortex K-ratios ranged 0.30 to 1.42 (mean: 0.68), indicating variable unidirectional AMT uptake in meningiomas. In contrast, AMT k_3' values in all meningiomas were lower than cortical k_3' ; the mean tumor/cortex ratio was 0.32 (range: 0.09–0.69).

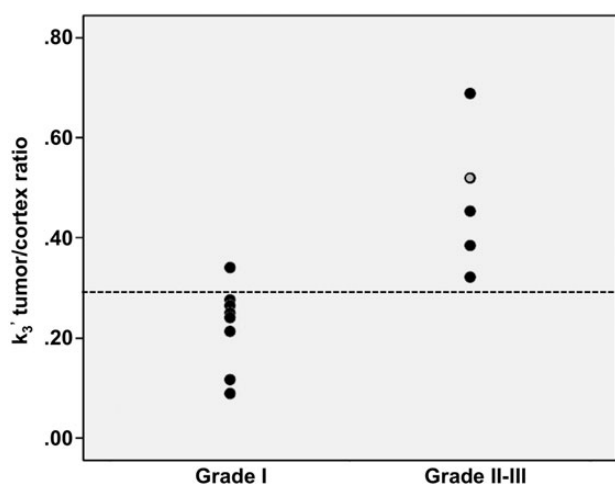
Comparison of Meningioma Grades and Correlations with Proliferative Activity

There was a strong positive correlation between meningioma grade and AMT k_3' tumor/cortex ratio ($r = 0.75$, $P = .003$). Positive correlations were also found between the Ki-67 proliferation

Table 1. Comparison of various AMT-PET parameters between the meningioma ($n = 16$), grade II glioma ($n = 21$), and grade III glioma ($n = 10$) subgroups. Ratios indicate tumor/contralateral cortex ratios of the PET parameters. P values refer to group comparisons (unpaired t tests) between the meningioma and glioma subgroups

AMT-PET Parameter	Meningiomas, Mean (SD)	Grade II Gliomas, Mean (SD)	P Value	Grade III Gliomas, Mean (SD)	P Value
SUV	3.99 (1.15)	3.20 (1.11)	.04	4.20 (1.56)	.71
SUV-ratio	1.61 (0.35)	1.54 (0.57)	.65	1.95 (0.61)	.09
VD'	0.82 (0.27)	0.38 (0.13)	<.001	0.84 (0.54)	.88
VD'-ratio	2.60 (0.79)	1.36 (0.66)	<.001	2.67 (1.05)	.87
K (mL/g/min)	0.0043 (0.0027)	0.0072 (0.0027)	.006	0.0068 (0.0027)	.04
K-ratio	0.78 (0.34)	1.77 (1.06)	.003	1.36 (0.31)	<.001
k_3' (min^{-1})	0.006 (0.004)	0.02 (0.008)	<.001	0.01 (0.005)	.04
k_3' -ratio	0.32 (0.16)	1.46 (1.09)	.001	0.59 (0.36)	.02

Abbreviations: K, AMT unidirectional uptake rate; k_3' , AMT metabolic rate; SD, standard deviation; SUV, standardized uptake value; VD', volume of distribution.

**Fig. 3.** WHO grade I meningiomas showed lower tumor/cortex k_3' -ratios than grade II-III meningiomas. A k_3' -ratio threshold of 0.3 (based on the ROC analysis; the threshold level is indicated by a dotted line) distinguished these 2 subgroups with 100% sensitivity and 88% specificity (92% accuracy). The value of the only grade III meningioma is indicated by the gray circle.

index (range: 1–15%) and tumor K ($r = 0.64$, $P = .019$), as well as tumor k_3' -values ($r = 0.54$, $P = .056$). A k_3' -ratio provided the best differentiating accuracy between grade I versus grade II-III meningiomas: using a ratio threshold of 0.3 (based on the ROC analysis, $AUC = 0.975$ [95% CI: 0.85–1]), these 2 subgroups could be distinguished with a 0.92 accuracy (95% CI: 0.85–1) (Fig. 3). Using this threshold, all but one meningioma was classified correctly to grade I versus II/III. There was no significant correlation between AMT parameters and age or tumor size ($P > .1$).

Comparison of Meningioma Versus Glioma Subgroups

Most kinetic parameters showed a robust difference between the meningioma and glioma subgroups (Table 1; Fig. 2). Specifically, K and tumor/cortex K-ratio, as well as k_3' and k_3' -ratio,

were higher in both low-grade and high-grade gliomas as compared with meningiomas; VD' and VD'-ratios were higher in meningiomas than in low-grade gliomas, while the difference was not significant when compared with high-grade gliomas (Table 1). Tumor/cortex k_3' -ratio provided the best accuracy to differentiate between low-grade gliomas and meningiomas. With a cutoff threshold of 0.71 ($AUC = 0.996$), we achieved 100% specificity and 95% sensitivity; all but one of the tumors were correctly classified (97% accuracy). For differentiation of meningiomas versus high-grade gliomas, the AMT K-ratio provided the best accuracy; a cutoff threshold of 1.01 ($AUC = 0.89$) achieved 90% sensitivity with 77% specificity (accuracy: 83%). AMT SUVs and SUV ratios were not different between meningiomas and the glioma subgroups, except for slightly higher SUVs in meningiomas as compared with low-grade gliomas (Table 1). Finally, we did not find any difference in tumor size between meningiomas and the 2 glioma groups ($P = .23$).

Immunostaining Patterns of the Kynurenine Pathway Enzymes

Among the 3 initial enzymes of the KP, TDO2 showed the highest immunostaining scores, followed by IDO2 and IDO1 (mean scores: 2 [range: 1–3], 1.5 [range: 0–3], and 0.5 [range: 0–1], respectively; Wilcoxon tests: TDO2 vs IDO2: $P = .048$; IDO2 vs IDO1: $P = .003$) (Fig. 4). Between the 2 downstream enzymes, KYNU showed the higher immunostaining scores as compared with KMO (mean: 2 [range: 0–2] vs 1.5 [1–3]; $P = .004$) (Fig. 4). In comparing the meningioma grades, TDO2 showed significantly higher immunostaining scores, while IDO2 showed a trend for stronger immunostaining in grade I meningiomas (Table 2).

Correlation between AMT-Positron Emission Tomography Parameters and Kynurenine Pathway Immunostaining Scores

There was a strong negative correlation of AMT k_3' tumor/cortex ratios with TDO2 immunostaining scores ($r = -0.79$, $P = .001$) and a marginal negative correlation with IDO1 scores ($r = -0.54$, $P = .06$).

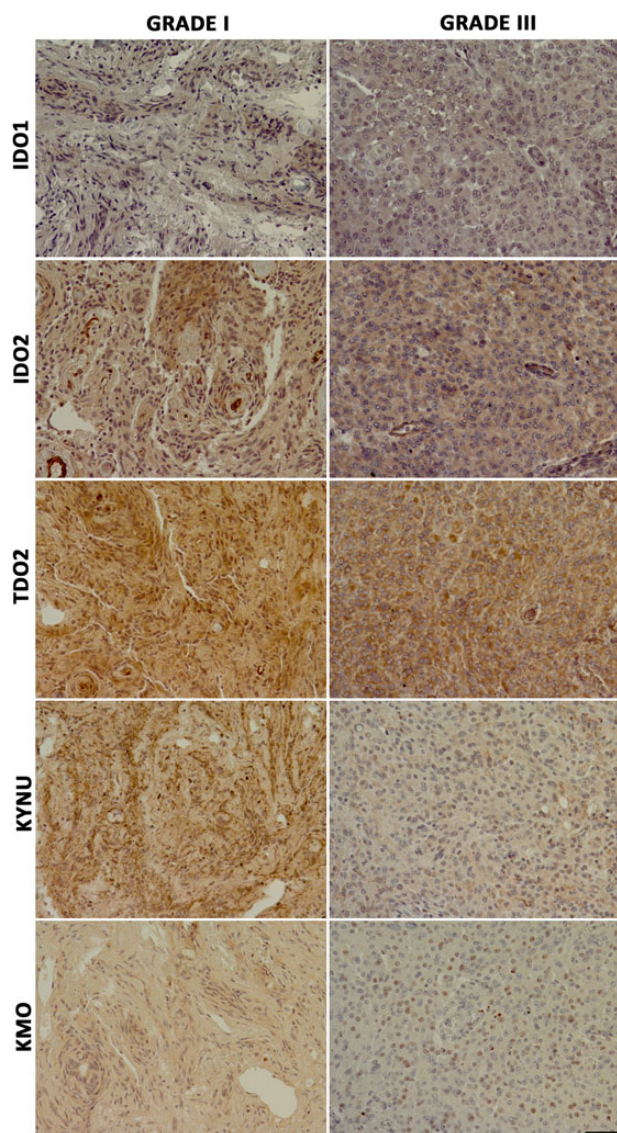


Fig. 4. Immunostaining for 5 key enzymes of the kynurenine pathway in a grade I and grade III meningioma. Both tumors showed TDO2>IDO2>IDO1 immunostaining. Between the 2 downstream enzymes, KYNU showed stronger staining as compared with KMO. The grade III meningioma showed overall weaker immunostaining for the same enzymes as compared with the grade I tumor. Original magnification 20 \times . The length of the scale bar is 50 μ m and applies to all images.

Discussion

This study describes 3 novel findings. First, AMT k_3' tumor/cortex ratios could distinguish grade I from grade II–III meningiomas. Second, AMT-PET kinetic parameters showed a striking difference between meningiomas and both grade II and grade III gliomas. These findings reinforce the significance of tracer kinetic analysis to enhance the clinical value of amino acid PET in the pretreatment evaluation of brain tumors. Finally, we found a prominent expression of TDO2 in addition to IDO1 and 2 in meningiomas, along with variable expression of

Table 2. Immunostaining scores of the 5 enzymes of the kynurenine pathway, compared between grade I ($n = 10$) and grade II–III ($n = 6$) meningiomas. P values refer to the results of the Mann-Whitney U test

Enzyme	Grade I Mean (SD)	Grade II–III Mean (SD)	P Value
IDO1	0.6 (0.5)	0.3 (0.5)	.36
IDO2	1.6 (0.8)	1.0 (0.5)	.07
TDO2	2.3 (0.7)	1.5 (0.5)	.04
KMO	1.6 (0.7)	1.8 (0.7)	.56
KYNU	2.4 (0.5)	2.2 (0.7)	.49

Abbreviations: IDO, indoleamine 2,3-dioxygenase; KMO, kynurenine 3-monooxygenase; KYNU, kynureninase; TDO, tryptophan 2,3-dioxygenase.

downstream KP enzymes. The strong correlation between TDO2 expression and AMT k_3' ratios suggests that TDO2 may be an important driver of *in vivo* tryptophan metabolism in these tumors. These findings could have important implications for developing effective drugs, such as KP enzyme inhibitors, to alter abnormal tryptophan metabolism in meningiomas and alleviate KP-induced tumoral immune tolerance.

Perhaps the most clinically important finding of our study is the high accuracy (92%) of AMT-PET for differentiating grade I versus grade II–III meningiomas. This accuracy appears to be much better than the differentiating accuracy reported for ^{11}C -methionine (MET)-PET. For example, a recent study did not find any correlation between methionine uptake and proliferative activity, microvessel density, and histological grade.⁴⁰ Other studies showed a significant correlation between proliferative activity and methionine uptake in meningiomas,^{41,42} but static MET uptake cannot reliably differentiate low-grade from high-grade meningiomas. A very recent preliminary PET study investigated the kinetic behavior of ^{18}F -fluoroethyl-L-tyrosine (FET) in meningiomas and then compared this with histological subtypes.⁴³ They found that FET tumor-to-brain ratios, measured in the late uptake phase (20–40 min) could differentiate low-grade from high-grade meningiomas with a sensitivity and specificity of 83%. Combination of ratios and the time-activity curve pattern improved the differentiating accuracy to 92%, which is similar to what we achieved by using AMT Patlak analysis. These results strongly suggest that tracer kinetic analysis is critical to achieving optimal pretreatment estimation of meningioma grade when using amino acid PET. Accurate estimation of meningioma grade can have a strong clinical impact for determining treatment options (eg, whether to proceed with surgery or opt for watchful waiting) with serial MRIs.

In our study, all meningiomas showed considerably higher tryptophan uptake (SUV) on PET when compared with AMT uptake in normal cortex. This is consistent with previous studies showing accumulation of other amino acid-based PET radiotracers in meningiomas.^{13,14,44,45} Because of the low background uptake in normal brain, amino acid PET generally allows better delineation of meningiomas compared with ^{18}F -fluoro-deoxy-glucose-PET.^{14,44} However, static amino acid uptake (SUV) has a limited value in further characterization of these tumors. Our data show that tracer kinetic parameters,

rather than SUVs, could differentiate meningiomas from both low-grade and high-grade gliomas. In our study, meningiomas could be differentiated from high-grade gliomas with 83% accuracy; the accuracy was even higher for low-grade gliomas (97%), although these are rarely mistaken for meningiomas. Pretreatment differentiation of these tumor types could significantly impact clinical management decisions and provide prognostic information in selected cases. While most meningiomas can be reliably identified on conventional MRI, up to 15% follow an atypical pattern.^{7,46} These morphological features can mimic a malignant glioma with necrotic changes. Thus, AMT-PET kinetic analysis may supplement MRI in selected cases to establish tumor type before treatment.

The exact processes underlying the striking difference in tryptophan kinetics in meningiomas versus gliomas remain unclear, but there are several potential mechanisms. High AMT VD' values, as found in meningiomas, indicate high net tryptophan transport rates from blood to tumor tissue. Meningiomas reside outside of the blood-brain barrier, and their strong vascularization, reflected by high regional cerebral blood volume on perfusion imaging,^{7,47} can lead to high tracer delivery. However, differences in blood-brain barrier do not fully explain tryptophan kinetic differences. While both SUV and VD' are known to be higher in contrast-enhancing brain tumors, AMT K and k_3' are much less affected by blood-brain barrier impairments.²⁴ This is supported by our results showing that both AMT K and k_3' parameters could differentiate meningiomas from high-grade gliomas, 2 groups that included many contrast-enhancing tumors. AMT k_3' values estimate the rate of AMT conversion to tryptophan metabolites that are trapped in the tumor compartment irreversibly. Strong expression of TDO2 (combined with IDO2 and, in some cases, IDO1), together with expression of downstream enzymes of the KP in grade I meningiomas can lead to an effective breakdown of tryptophan (and AMT) to downstream metabolites, assuming that the IHC-detected enzymes are active. This can lead to cleavage of the ¹¹C-methyl group, which could prevent radiotracer (AMT) accumulation and trapping. This is likely reflected by the lower AMT k_3' values found in low-grade meningiomas. This mechanism is also supported by the strong negative correlation between TDO2 expression and AMT k_3' ratios.

The preferential expression of TDO2 in meningiomas is a novel finding that certainly deserves further attention. In previous studies, TDO2 was found to be expressed in malignant gliomas, with or without co-expression of IDO1 or IDO2.³⁰ We have also previously reported strong IDO expression in some low-grade gliomas and glioneuronal tumors,^{15,21} where IDO-induced tumoral immune tolerance may be advantageous to achieving long-term survival and growth in the host micro-environment. However, prominent TDO2 expression has not been reported in low-grade brain tumors before. Our results suggest that TDO2 may play a key role in conversion of tryptophan to kynurenine and downstream metabolites in meningiomas, potentially contributing to tumor-induced immunosuppression. The effect of TDO2 (and other KP enzymes) on immune cells infiltrating meningiomas should be assessed in future studies. Nevertheless, our tissue results support the notion that selective inhibition of IDO1/2 or TDO2 may not be effective in completely blocking the first step of the KP. Rather, optimal KP blockade may require an individualized approach

or use of an omnipotent IDO/TDO inhibitor.³¹ This will require further detailed characterization of the activity of KP enzymes and KP metabolites in different brain tumor types.

Our study has several limitations. First, we had a relatively small group of meningioma patients with a limited number of high-grade tumors. Therefore, the differentiating accuracy of tryptophan PET should be confirmed in larger cohorts. Another limitation is the scarce availability of AMT in other centers. Although AMT has been used in centers in North America and Europe,³⁸ the short half-life of AMT (similar to MET) precludes the convenient and widespread clinical use of this radiotracer. However, interest in molecular imaging techniques targeting the KP has clearly been growing recently as the KP enzyme inhibitors (eg, the IDO inhibitors indoximod and INCB24360) have entered clinical trials. While our AMT-PET studies provide proof-of-principle data, it is quite possible that more widespread clinical applications will be pursued with other recently developed F-18-labeled radiotracers targeting tryptophan transport and/or metabolism via the kynurenine pathway (such as an F-18-labeled IDO1 inhibitor⁴⁸ or various tryptophan derivatives^{49,50}).

In conclusion, we have demonstrated that kinetic analysis of AMT uptake by PET allows accurate differentiation of low-grade versus high-grade meningiomas, thus facilitating optimal management decisions. In addition, the presence of multiple KP enzymes in these tumors supports the feasibility of pharmacological targeting of the KP, including TDO2, which appears to play a role (in addition to IDO1 and IDO2) in abnormal tryptophan metabolism in meningiomas. However, further studies are required to determine the role of the KP in meningioma immune tolerance. Molecular imaging with AMT or other radiotracers targeting the KP could be instrumental for monitoring in vivo treatment effects in future clinical trials with KP enzyme inhibitors.

Funding

The study was supported by a grant (R01 CA123451 to C.J. and S.M.) from the National Cancer Institute; a grant from the Fund for Medical Research and Education, Wayne State University School of Medicine (to S.M.); and Strategic Research Initiative Grant from the Karmanos Cancer Institute (to S.M. and C.J.). Tissue sections were prepared by the Biobanking and Correlative Sciences Core, which is supported in part by NIH Center grant P30 CA022453 to the Karmanos Cancer Institute at Wayne State University.

Acknowledgments

We thank Geoffrey Barger, MD, Kelly Forcucci, RN, Janet Barger, RN, and Cathie Germain, MA for assisting with patient recruitment and scheduling. We also thank James Janisse, PhD, for assisting with the statistical analysis and Kiara P. Brooks, BS, for assistance with the tissue staining. We are grateful to the entire staff at the PET Center, Children's Hospital of Michigan, who provided invaluable technical help in performing the PET scans.

Conflict of interest statement. None of the authors report any conflict of interest or financial disclosure.

References

- Wiemels J, Wrensch M, Claus EB. Epidemiology and etiology of meningioma. *J Neurooncol*. 2010;99(3):307–314.
- Yano S, Kuratsu J, Kumamoto Brain Tumor Research Group. Indications for surgery in patients with asymptomatic meningiomas based on an extensive experience. *J Neurosurg*. 2006;105(4):538–543.
- Cha S. Neuroimaging in neuro-oncology. *Neurotherapeutics*. 2009;6(3):465–477.
- Smith JK, Castillo M, Kwock L. MR spectroscopy of brain tumors. *Magn Reson Imaging Clin N Am*. 2003;11(3):415–429.
- Filss CP, Galdiks N, Stoffels G, et al. Comparison of ¹⁸F-FET PET and perfusion-weighted MR imaging: a PET/MR imaging hybrid study in patients with brain tumors. *J Nucl Med*. 2014;55(4):540–545.
- Chernov MF, Kasuya H, Nakaya K, et al. ¹H-MRS of intracranial meningiomas: what it can add to known clinical and MRI predictors of the histopathological and biological characteristics of the tumor? *Clin Neural Neurosurg*. 2011;113(3):202–212.
- Harting I, Hartmann M, Bonsanto MM, et al. Characterization of necrotic meningioma using diffusion MRI, perfusion MRI, and MR spectroscopy: case report and review of the literature. *Neuroradiology*. 2004;46(3):189–193.
- Jain A, Hoepflich M, Mittal M, et al. Spontaneous intratumoral infarction - an unusual evolution of a falxine meningioma. *Clin Neuropathol*. 2014;33(6):412–417.
- Dhermain FG, Hau P, Lanfermann H, et al. Advanced MRI and PET imaging for assessment of treatment response in patients with gliomas. *Lancet Neurol*. 2010;9(9):906–920.
- Zhang H, Rodiger LA, Shen T, et al. Perfusion MR imaging for differentiation of benign and malignant meningiomas. *Neuroradiology*. 2008;50(6):525–530.
- Sanverdi SE, Ozgen B, Oguz KK, et al. Is diffusion-weighted imaging useful in grading and differentiating histopathological subtypes of meningiomas? *Eur J Radiol*. 2012;81(9):2389–2395.
- Chen W. Clinical applications of PET in brain tumors. *J Nucl Med*. 2007;48:1468–1481.
- Rutten I, Cabay JE, Withofs N, et al. PET/CT of skull base meningiomas using 2-¹⁸F-fluoro-L-tyrosine: initial report. *J Nucl Med*. 2007;48(9):720–725.
- Ikeda H, Tsuyuguchi N, Kunihiro N, et al. Analysis of progression and recurrence of meningioma using (11)C-methionine PET. *Ann Nucl Med*. 2013;27(8):772–780.
- Alkonyi B, Mittal S, Zitron I, et al. Increased tryptophan transport in epileptogenic dysembryoplastic neuroepithelial tumors. *J Neurooncol*. 2012;107(2):365–372.
- Juhász C, Nahleh Z, Zitron I, et al. Tryptophan metabolism in breast cancers: molecular imaging and immunohistochemistry studies. *Nucl Med Biol*. 2012;39(7):926–932.
- Haining Z, Kawai N, Miyake K, et al. Relation of LAT1/4F2hc expression with pathological grade, proliferation and angiogenesis in human gliomas. *BMC Clin Pathol*. 2012;12:4.
- Diksic M, Nagahiro S, Sourkes TL, et al. A new method to measure brain serotonin synthesis in vivo. I. Theory and basic data for a biological model. *J Cereb Blood Flow Metab*. 1990;10(1):1–12.
- Chugani DC, Muzik O. Alpha-[¹¹C]methyl-L-tryptophan PET maps brain serotonin synthesis and kynurenine pathway metabolism. *J Cereb Blood Flow Metab*. 2000;20(1):2–9.
- Munn DH, Mellor AL. Indoleamine 2,3-dioxygenase and tumor-induced tolerance. *J Clin Invest*. 2007;117(5):1147–1154.
- Batista CE, Juhász C, Muzik O, et al. Imaging correlates of differential expression of indoleamine 2,3-dioxygenase in human brain tumors. *Mol Imaging Biol*. 2009;11(6):460–466.
- Miyazaki T, Moritake K, Yamada K, et al. Indoleamine 2,3-dioxygenase as a new target for malignant glioma therapy. *Laboratory investigation*. *J Neurosurg*. 2009;111(2):230–237.
- Wainwright DA, Balyasnikova IV, Chang AL, et al. IDO expression in brain tumors increases the recruitment of regulatory T cells and negatively impacts survival. *Clin Cancer Res*. 2012;18(22):6110–6121.
- Juhász C, Chugani DC, Muzik O, et al. In vivo uptake and metabolism of alpha-[¹¹C]methyl-L-tryptophan in human brain tumors. *J Cereb Blood Flow Metab*. 2006;26(3):345–357.
- Juhász C, Muzik O, Chugani DC, et al. Differential kinetics of alpha-[¹¹C]methyl-L-tryptophan on PET in low-grade brain tumors. *J Neurooncol*. 2011;102(3):409–415.
- Alkonyi B, Barger GR, Mittal S, et al. Accurate differentiation of recurrent gliomas from radiation injury by kinetic analysis of alpha-¹¹C-methyl-L-tryptophan PET. *J Nucl Med*. 2012;53(7):1058–1064.
- Juhász C, Chugani DC, Barger GR, et al. Quantitative PET imaging of tryptophan accumulation in gliomas and remote cortex: correlation with tumor proliferative activity. *Clin Nucl Med*. 2012;37(9):838–842.
- Kamson DO, Mittal S, Robinette NL, et al. Increased tryptophan uptake on PET has strong independent prognostic value in patients with a previously treated high-grade glioma. *Neuro Oncol*. 2014;16(10):1373–1383.
- Zitron IM, Kamson DO, Kioussis S, et al. In vivo metabolism of tryptophan in meningiomas is mediated by indoleamine 2,3-dioxygenase 1. *Cancer Biol Ther*. 2013;14(4):333–339.
- Opitz CA, Litzenburger UM, Sahm F, et al. An endogenous tumour-promoting ligand of the human aryl hydrocarbon receptor. *Nature*. 2011;478(7368):197–203.
- Austin CJ, Rendina LM. Targeting key dioxygenases in tryptophan-kynurenine metabolism for immunomodulation and cancer chemotherapy. *Drug Discov Today*. 2015;20(5):609–617.
- Chakraborty PK, Mangner TJ, Chugani DC, et al. A high-yield and simplified procedure for the synthesis of alpha-[¹¹C]methyl-L-tryptophan. *Nucl Med Biol*. 1996;23(8):1005–1008.
- Patlak CS, Blasberg RG, Fenstermacher JD. Graphical evaluation of blood-to-brain transfer constants from multiple-time uptake data. *J Cereb Blood Flow Metab*. 1983;3(1):1–7.
- Juhász C, Muzik O, Lu X, et al. Quantification of tryptophan transport and metabolism in lung tumors using PET. *J Nucl Med*. 2009;50(3):356–363.
- Muzik O, Chugani DC, Chakraborty P, et al. Analysis of [¹¹C]alpha-methyl-tryptophan kinetics for the estimation of serotonin synthesis rate in vivo. *J Cereb Blood Flow Metab*. 1997;17(6):659–669.
- Juhász C, Dwivedi S, Kamson DO, et al. Comparison of amino acid positron emission tomographic radiotracers for molecular imaging of primary and metastatic brain tumors. *Mol Imaging*. 2014;13: doi:10.2310/7290.2014.00015.
- Kikinis R, Pieper S. 3D Slicer as a tool for interactive brain tumor segmentation. *Conf Proc IEEE Eng Med Biol Soc*. 2011;2011:6982–6984.

38. Mattes D, Haynor DR, Vesselle H, et al. PET-CT image registration in the chest using free-form deformations. *IEEE Trans Med Imaging*. 2003;22(1):120–128.
39. Robin X, Turck N, Hainard A, et al. pROC: an open-source package for R and S+ to analyze and compare ROC curves. *BMC Bioinformatics*. 2011;12:77.
40. Arita H, Kinoshita M, Okita Y, et al. Clinical characteristics of meningiomas assessed by ¹¹C-methionine and ¹⁸F-fluorodeoxy glucose positron-emission tomography. *J Neurooncol*. 2012; 107(2):379–386.
41. Iuchi T, Iwadate Y, Namba H, et al. Glucose and methionine uptake and proliferative activity in meningiomas. *Neur Res*. 1999;21(7):640–644.
42. Chung JK, Kim YK, Kim SK, et al. Usefulness of ¹¹C-methionine PET in the evaluation of brain lesions that are hypo- or isometabolic on ¹⁸F-FDG PET. *Eur J Nucl Med Imaging*. 2002;29(2):176–182.
43. Cornelius JF, Stoffels G, Filss C, et al. Uptake and tracer kinetics of O-(2-(¹⁸F)-fluoroethyl)-L-tyrosine in meningiomas: preliminary results. *Eur J Nucl Med Imaging*. 2015;42(3):459–467.
44. Cornelius JF, Langen KJ, Stoffels G, et al. Positron emission tomography imaging of meningioma in clinical practice: review of literature and future directions. *Neurosurgery*. 2012;70(4):1033–1041.
45. Aki T, Nakayama N, Yonezawa S, et al. Evaluation of brain tumors using dynamic ¹¹C-methionine-PET. *J Neurooncol*. 2012;109(1): 115–122.
46. Buetow MP, Buetow PC, Smirniotopoulos JG. Typical, atypical, and misleading features in meningioma. *Radiographics*. 1991;11(6): 1087–1106.
47. Kremer S, Grand S, Remy C, et al. Cerebral blood volume mapping by MR imaging in the initial evaluation of brain tumors. *J Neuroradiol*. 2002;29(2):105–113.
48. Huang X, Gillies RJ, Tian H. Synthesis of [¹⁸F] 4-amino-N-(3-chloro-4-fluorophenyl)-N'-hydroxy-1,2,5-oxadiazole-3-carboximid amide (IDO5L): a novel potential PET probe for imaging of IDO1 expression. *J Labelled Comp Radiopharm*. 2015;58(4): 156–162.
49. Chiotellis A, Mu L, Muller A, et al. Synthesis and biological evaluation of ¹⁸F-labeled fluoropropyl tryptophan analogs as potential PET probes for tumor imaging. *Eur J Med Chem*. 2013; 70:768–780.
50. Chiotellis A, Muller A, Mu L, et al. Synthesis and biological evaluation of (¹⁸F)-labeled Fluoroethoxy tryptophan analogues as potential PET tumor imaging agents. *Mol Pharm*. 2014; 11(11):3839–3851.